

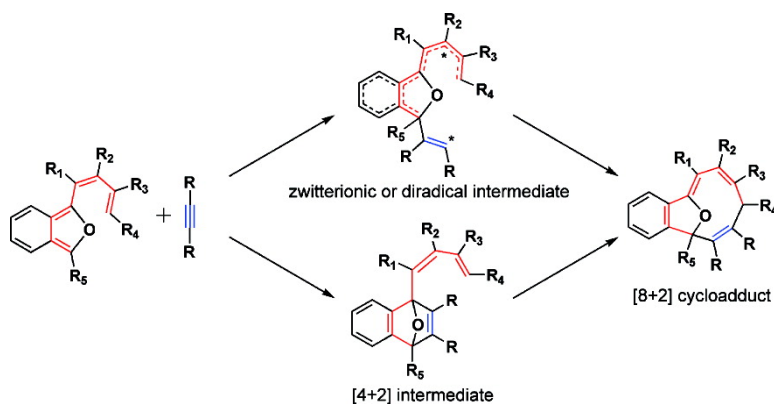
Article

Mechanistic Twist of the [8+2] Cycloadditions of Dienylisobenzofurans and Dimethyl Acetylenedicarboxylate: Stepwise [8+2] versus [4+2]/[1,5]-Vinyl Shift Mechanisms Revealed through a Theoretical and Experimental Study

Yuanyuan Chen, Siyu Ye, Lei Jiao, Yong Liang, Dilip K. Sinha-Mahapatra, James W. Herndon, and Zhi-Xiang Yu

J. Am. Chem. Soc., **2007**, 129 (35), 10773-10784 • DOI: 10.1021/ja072203u • Publication Date (Web): 14 August 2007

Downloaded from <http://pubs.acs.org> on February 15, 2009



More About This Article

Additional resources and features associated with this article are available within the HTML version:

- Supporting Information
- Links to the 4 articles that cite this article, as of the time of this article download
- Access to high resolution figures
- Links to articles and content related to this article
- Copyright permission to reproduce figures and/or text from this article

[View the Full Text HTML](#)



ACS Publications
 High quality. High impact.

Mechanistic Twist of the [8+2] Cycloadditions of Dienylisobenzofurans and Dimethyl Acetylenedicarboxylate: Stepwise [8+2] versus [4+2]/[1,5]-Vinyl Shift Mechanisms Revealed through a Theoretical and Experimental Study

Yuanyuan Chen,[†] Siyu Ye,[†] Lei Jiao,[†] Yong Liang,[†] Dilip K. Sinha-Mahapatra,[‡] James W. Herndon,[‡] and Zhi-Xiang Yu^{*†}

Contribution from the Beijing National Laboratory for Molecular Sciences (BNLMS), Key Laboratory of Bioorganic Chemistry and Molecular Engineering of the Ministry of Education, College of Chemistry, Peking University, Beijing 100871, People's Republic of China, and Department of Chemistry and Biochemistry, New Mexico State University, MSC 3C, Las Cruces, New Mexico 88003

Received March 29, 2007; E-mail: yuzx@pku.edu.cn

Abstract: Recently, it was reported that both dienyfurans and dienyisobenzofurans could react with dimethyl acetylenedicarboxylate (DMAD) to give [8+2] cycloadducts. Understanding these [8+2] reactions will aid the design of additional [8+2] reactions, which have the potential for the synthesis of 10-membered and larger carbocycles. The present Article is aimed to understand the detailed mechanisms of the originally reported [8+2] cycloaddition reaction between dienyisobenzofurans and alkynes at the molecular level through the joint forces of computation and experiment. Density functional theory calculations at the (U)-B3LYP/6-31+G(d) level suggest that the concerted [8+2] pathway between dienyisobenzofurans and alkynes is not favored. A stepwise reaction pathway involving formation of a zwitterionic intermediate for the [8+2] reactions between dienyisobenzofurans that contain electron-donating methoxy groups present in their diene moieties and DMAD has been predicted computationally. This pathway is in competition with a Diels–Alder [4+2] reaction between the furan moieties of dienyisobenzofurans and DMAD. When there is no electron-donating group present in the diene moieties of dienyisobenzofurans, the [8+2] reaction occurs through an alternative mechanism involving a [4+2] reaction between the furan moiety of the tetraene and DMAD, followed by a [1,5]-vinyl shift. This computationally predicted novel mechanism was supported experimentally.

1. Introduction

Orbital-symmetry allowed [8+2] cycloadditions between tetraenes and tetraenophiles can in theory provide a straightforward approach for the synthesis of 10-membered ring compounds.^{1–4} Before the year 2003, however, all of the reported [8+2] cycloadditions were limited to geometrically constrained tetraenes such as heptafulvenes, tropones, and indolizines, in which the terminal carbons or heteroatoms at positions 1 and 8 are rigidly held in close proximity (Scheme 1, reactions a and b). Consequently, only bicyclic or tricyclic compounds instead of 10-membered ring compounds were obtained in these [8+2] cycloadditions. The only reported [8+2] cycloaddition employing geometrically flexible tetraenes in the last century is the reaction between 1,6-dimethylene cyclohepta-

2,4-diene and tetraenophiles such as tetracyanoethylene and dimethyl azodicarboxylate^{4h} (Scheme 1, reaction c). Development of new [8+2] cycloadditions between geometrically flexible tetraenes and tetraenophiles can result in new and highly convergent synthetic approaches to 10-membered ring compounds.^{5,6}

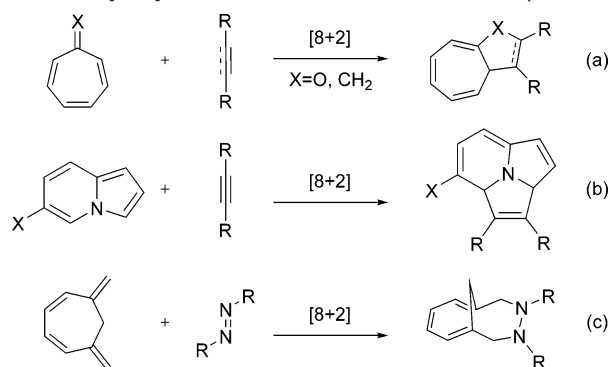
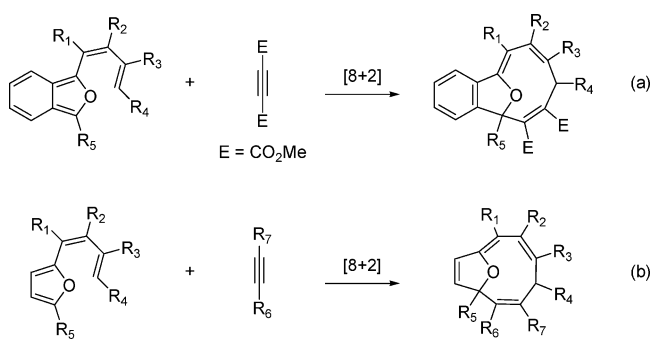
In 2003, it was reported that dienyisobenzofurans can react with dimethyl acetylenedicarboxylate (DMAD) to furnish [8+2] adducts possessing the 11-oxabicyclo[6.2.1]undecane ring system as the major products (Scheme 2, reaction a).^{7a} It was later noted that dienyfurans could also participate in the [8+2]

[†] Peking University.

[‡] New Mexico State University.

- (1) The first reported [8+2] cycloaddition: Doering, W. v. E.; Wiley, D. W. *Tetrahedron* **1960**, *11*, 183.
- (2) (a) Woodward, R. B.; Hoffmann, R. *The Conservation of Orbital Symmetry*; Verlag Chemie/Academic Press: Weinheim, 1971. (b) Woodward, R. B.; Hoffmann, R. *Angew. Chem., Int. Ed. Engl.* **1969**, *8*, 781.
- (3) For a review of [8+2] cycloaddition, see: Nair, V.; Anilkumar, G. *Synlett* **1998**, 950.

- (4) For other selected [8+2] cycloadditions, see: (a) Liu, C. Y.; Mareda, J.; Houk, K. N.; Fronczek, F. R. *J. Am. Chem. Soc.* **1983**, *105*, 6714. (b) Liu, C. Y.; Ding, S. T. *J. Org. Chem.* **1992**, *57*, 4539. (c) Liu, C. Y.; Houk, K. N. *Tetrahedron Lett.* **1987**, *28*, 1371. (d) Daub, J.; Hirmer, G.; Kakob, L.; Maas, G.; Pickl, W.; Pirzer, E.; Rapp, K. M. *Chem. Ber.* **1985**, *118*, 1836. (e) Bäumler, A.; Daub, J.; Pickl, W.; Rieger, W. *Chem. Ber.* **1985**, *118*, 1857. (f) Hayakawa, K.; Nishiyama, H.; Kanematsu, K. *J. Org. Chem.* **1985**, *50*, 512. (g) Kumar, K.; Kapur, A.; Ishar, M. P. S. *Org. Lett.* **2000**, *2*, 787. (h) Farrant, G. C.; Feldmann, R. *Tetrahedron Lett.* **1970**, *11*, 4979. (i) Komatsu, K.; Fujimori, M.; Okamoto, K. *Tetrahedron* **1977**, *33*, 2791. (j) Pham, W.; Weissleder, R.; Tung, C. H. *Tetrahedron Lett.* **2002**, *43*, 19. (k) Nair, V.; Anilkumar, G.; Nandakumar, M. V.; Mathew, B.; Rath, N. P. *Tetrahedron Lett.* **1997**, *38*, 6441. (l) Babaev, E. V.; Simonyan, V. V.; Pasichnichenko, K. Y.; Nosova, V. M.; Kisin, A. V.; Jug, K. *J. Org. Chem.* **1999**, *64*, 9057.

Scheme 1. [8+2] Reactions of Tetraenes with Tetraenophiles**Scheme 2.** [8+2] Reactions Reported by Herndon and Co-workers

cycloadditions with DMAD (Scheme 2, reaction b).^{7b} These [8+2] cycloadditions provide a direct approach for the synthesis of ring skeletons of eleutherobin, briarellins, and other natural products that have anticancer activity.^{5,6} As compared to [8+2] cycloadditions using geometrically constrained tetraenes, the [8+2] cycloaddition reactions highlighted in Scheme 2 employ flexible tetraenes in which the terminal C1 and C8 are not held in close proximity. More importantly, 10-membered ring compounds with an oxygen bridge can be readily synthesized through these [8+2] cycloadditions. Understanding the mechanisms of these [8+2] cycloadditions will not only enhance knowledge of [8+2] cycloaddition reactions and the chemistry of pericyclic reactions, but also provide insights and guides for the future design of new [8+2] and other higher order [*m*+*n*] cycloadditions that have the potential application in the synthesis of 10-membered or larger ring compounds.

Likely mechanisms for the formation of [8+2] cycloadducts between dienylobenzofuran and DMAD are depicted in Scheme 3. These pathways include a concerted [8+2] cycloaddition (pathway A) or a stepwise pathway B involving the formation of a zwitterionic (or diradical) intermediate. These two pathways can be easily proposed if one considers the

mechanisms of Diels–Alder reactions, which occur via either a concerted or a stepwise pathway.⁸ In addition to pathways A and B, we propose a novel pathway C for the [8+2] cycloaddition (Scheme 3). Pathway C begins with a [4+2] cycloaddition of DMAD and the furan moiety of the tetraene to give a [4+2] cycloadduct, which then isomerizes via a [1,5]-vinyl shift to furnish the final [8+2] cycloadduct.^{9,10} If [8+2] cycloadditions occur via pathway C and this could be verified experimentally, it is likely that any bicyclo[2.2.1]heptene system, easily obtained through Diels–Alder chemistry, could be transformed to a 10-membered ring system after installation of the exocyclic diene group. We envisioned that such a ring-enlargement strategy could also be applied to the construction of other large ring compounds.

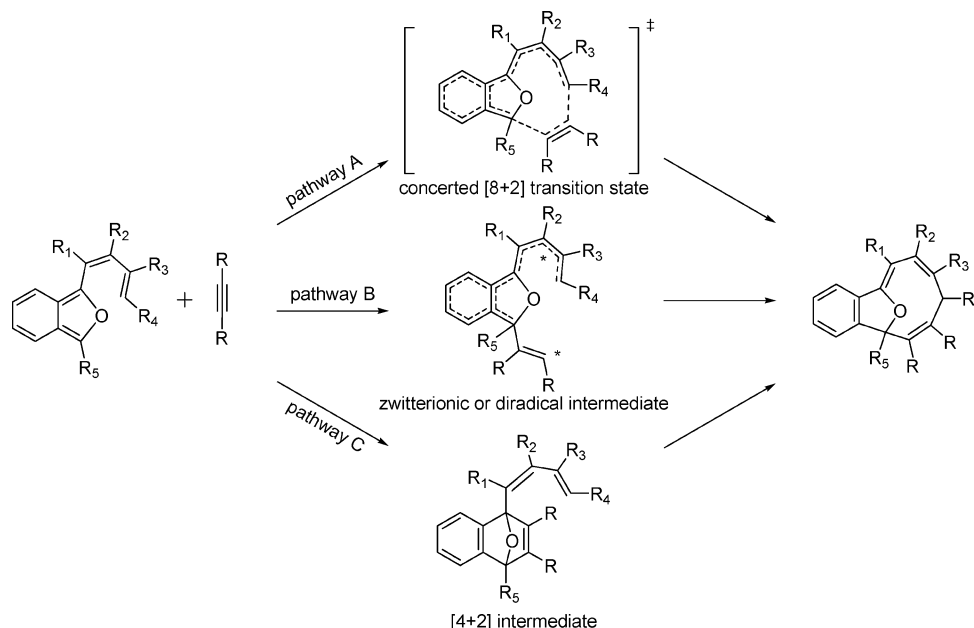
With the above-mentioned mechanistic objectives in mind,¹⁰ especially to test whether pathway C is feasible or not, a theoretical and experimental study of the [8+2] cycloadditions of dienylobenzofurans and DMAD has been performed. These results show that pathway A is not favored intrinsically (see discussions below). Pathways B and C are possible, and their preference varies, depending on the substituents present in the tetraene substrates. When there is no electron-donating group (such as methoxy group) in the dienyli moiety of dienylobenzofurans, the favored pathway for the [8+2] reaction is pathway C via the [4+2]/[1,5]-vinyl shift mechanism. When an electron-donating group such as the methoxy group is present in the dienyli moiety of dienylobenzofurans, pathway C is still favored in gas phase but pathway B is very competitive in solution because the methoxy group can stabilize the zwitterionic transition states and intermediates involved in pathway B more significantly than those stationary points in pathway C. In this Article, detailed theoretical and experimental studies that explore the whole scenario of mechanistic twists of [8+2] cycloadditions between dienylobenzofurans and DMAD are presented.

2. Computational Methodologies

All of the calculations were performed with the Gaussian 03 program.¹¹ The hybrid B3LYP functional¹² in conjunction with the 6-31+G(d) basis set¹³ was applied for the optimization of all of the stationary points in gas phase.^{14–17} A basis set that includes diffuse functions for heavy atoms better describes the zwitterionic species in these reactions. Singlet diradical transition states and intermediates were

(5) For a review of 10-membered ring natural compounds, see: (a) Bernardelli, P.; Paquette, L. *Heterocycles* **1998**, *49*, 531. The most important compound in this class is the potential anticancer agent eleutherobin, see: (b) Lindel, T.; Jensen, P. R.; Fenical, W.; Long, B. H.; Casazza, A. M.; Carboni, J.; Fairchild, C. R. *J. Am. Chem. Soc.* **1997**, *119*, 8744. (c) Lindel, T. *Angew. Chem., Int. Ed.* **1998**, *37*, 774.
(6) The synthesis of 10-membered ring compounds could also be achieved via [6+4] cycloadditions, see: (a) Houk, K. N.; Woodward, R. B. *J. Am. Chem. Soc.* **1970**, *92*, 4143. (b) Houk, K. N.; Woodward, R. B. *J. Am. Chem. Soc.* **1970**, *92*, 4145. (c) Bhacca, N. S.; Luskus, L. J.; Houk, K. N. *Chem. Commun.* **1971**, 109. (d) For a recent theoretical study of [6+4] cycloaddition, see: Leach, A. G.; Goldstein, E.; Houk, K. N. *J. Am. Chem. Soc.* **2003**, *125*, 8330.
(7) (a) Luo, Y.; Herndon, J. W.; Cervantes-Lee, F. *J. Am. Chem. Soc.* **2003**, *125*, 12720. (b) Zhang, L.; Wang, Y.; Buckingham, C.; Herndon, J. W. *Org. Lett.* **2005**, *7*, 1665.

(8) For studies of the mechanisms of Diels–Alder reactions, see: (a) Houk, K. N.; Gonzalez, J.; Li, Y. *Acc. Chem. Res.* **1995**, *28*, 81. (b) Houk, K. N.; Li, Y.; Evanseck, J. D. *Angew. Chem., Int. Ed. Engl.* **1992**, *31*, 682. (c) Goldstein, E.; Beno, B.; Houk, K. N. *J. Am. Chem. Soc.* **1996**, *118*, 6036. (d) Barriault, L.; Thomas, J. D. O.; Clement, R. *J. Org. Chem.* **2003**, *68*, 2317. (e) Rodriguez, D.; Navarro-Vazquez, A.; Castedo, L.; Dominguez, D.; Saa, C. *J. Am. Chem. Soc.* **2001**, *123*, 9178. (f) Sakai, S. *J. Phys. Chem. A* **2000**, *104*, 922. (g) Valley, N. A.; Wiest, O. *J. Org. Chem.* **2007**, *72*, 559. (h) Kong, S.; Evanseck, J. D. *J. Am. Chem. Soc.* **2000**, *122*, 10418.
(9) For theoretical studies of [1,5]-vinyl shift, see: (a) Kläner, F.-G.; Ehrhardt, R.; Bandmann, H.; Boese, R.; Bläser, D.; Houk, K. N.; Beno, B. R. *Chem.-Eur. J.* **1999**, *5*, 2119. (b) Alder, R. W.; Grimme, W. *Tetrahedron* **1981**, *37*, 1809. For reactions involving [1,5]-vinyl shift, see: (c) Semmelhack, M. F.; Weller, H. N.; Foes, J. S. *J. Am. Chem. Soc.* **1977**, *99*, 292. (d) Semmelhack, M. F.; Weller, H. N.; Clardy, J. *J. Org. Chem.* **1978**, *43*, 3791. (e) Fräter, G.; Müller, U. *Helv. Chim. Acta* **1988**, *71*, 808.
(10) There is another possible pathway D, which starts from [4+2] cycloaddition of alkyne to the dienyli moiety of isobenzofuran, followed by [1,5]-vinyl shift. Such pathway was proved to be very difficult because the computed [1,5]-vinyl shift step requires an activation energy more than 73 kcal/mol. See the Supporting Information for details.
(11) Frisch, M. J.; et al. *Gaussian 03*, revision C.02; Gaussian, Inc.: Wallingford, CT, 2004.
(12) (a) Becke, A. D. *J. Chem. Phys.* **1993**, *98*, 5648. (b) Lee, C.; Yang, W.; Parr, R. G. *Phys. Rev. B* **1988**, *37*, 785.
(13) Hehre, W. J.; Radom, L.; Schleyer, P. v. R.; Pople, J. A. *Ab Initio Molecular Orbital Theory*; Wiley: New York, 1986.

Scheme 3. Three Possible Pathways for Dienylisobenzofuran-Alkyne [8+2] Cycloaddition

located with UB3LYP/6-31+G(d). Frequency calculations were performed to confirm that each stationary point is either a minimum or a transition structure. In cases where transition structures are not easily confirmed by animation of their negative vibrations, IRC¹⁸ calculations were used to confirm the connection between the reactant, product, and transition state, which are given in the Supporting Information. The wavefunctions of several key diradical and zwitterionic stationary points in model reactions I and II have been computationally tested as stable ones. The reported relative energies are free energies (ΔG), enthalpies (ΔH , given in the Supporting Information), and zero-point energy (ZPE)-corrected electronic energies (ΔE_0) in gas phase. Solvent effects in benzene were computed by the CPCM model¹⁹ using the gas-phase optimized structures (using keyword: RADII=UAHF). The computed activation free energies in solution, referred to as ΔG_{sol} , were calculated by adding the solvation energies to the computed gas-phase relative free energies. The molecular orbital energies were computed at the HF/6-31G(d) level based on the B3LYP/6-31+G(d) geometries in gas phase. The spin density distribution of all of the diradical stationary points is provided in the Supporting Information. Unless otherwise specified, all discussed relative energies refer to the gas-phase calculations.

3. Results and Discussion

To fully understand the mechanisms of the [8+2] reactions between dienylisobenzofurans and DMAD and the mechanistic

twists caused by substituents in the dienyl moieties of dienylisobenzofurans, model reactions I–IV shown in Scheme 4 have been studied computationally. Experiments that test the theoretical predictions have also been conducted. First, the theoretical study of the [8+2] reaction between dienylisobenzofuran and acetylene will be presented to understand the inherent reaction preferences of [8+2] over [4+2] in this parent system (section 3.1). In section 3.2, a theoretical study of model reaction II will be presented to show the preference using tetraenophiles of appropriate reactivities. After presenting this theoretical prediction, we will then provide experimental evidence to support our prediction. Furthermore, in this part, we have also obtained the kinetic data to corroborate experimental and computational activation parameters, showing that B3LYP/6-31+G(d) is very suitable for the mechanistic investigation of the present [8+2] cycloadditions.^{20–22} In section 3.3, we will present theoretical studies of model reactions III and IV, demonstrating that the presence of a methoxy group makes the stepwise zwitterionic pathway B competitive with pathway C. This mechanism in model reactions III and IV has also been tested and supported experimentally.

3.1. Theoretical Study of Model Reaction I of Dienylisobenzofuran and Acetylene. Figure 1 shows the DFT computed energy surfaces for pathways B and C of model

- (14) Spin contamination is well known for the calculations of singlet diradical species. We have also computed the spin contamination for all singlet diradical stationary points using the Yamaguchi–Houk spin projection method^{15a} (see the Supporting Information for details). It was found that the computed activation energy without Yamaguchi–Houk correction for the vinyl shift step of **19** to **21** is close to the experimentally measured one, whereas the computed activation energy after Yamaguchi–Houk correction is lower by about 4 kcal/mol than the experimentally measured one. Due to this, the reported energies in this Article for all singlet diradical stationary points have not been corrected using the Yamaguchi–Houk spin projection method.^{15b}
- (15) (a) Yamaguchi, K.; Jensen, F.; Dorigo, A.; Houk, K. N. *Chem. Phys. Lett.* **1988**, *149*, 537. (b) For comments on the spin projection method, see: Wittbrodt, J. M.; Schlegel, H. B. *J. Chem. Phys.* **1996**, *105*, 6574.
- (16) We found that the UMP2 method is not suitable for the investigation of [1,5]-vinyl shift reaction. This is because the UHF wavefunction for the vinyl shift transition state is not stable; consequently, the UMP2 energy based on this wavefunction is questionable.¹⁷
- (17) Carsky, P.; Hubak, E. *Theor. Chim. Acta* **1991**, *80*, 407.
- (18) (a) Fukui, K. *J. Phys. Chem.* **1970**, *74*, 4161. (b) Gonzalez, C.; Schlegel, H. B. *J. Chem. Phys.* **1989**, *90*, 2154. (c) Gonzalez, C.; Schlegel, H. B. *J. Phys. Chem.* **1990**, *94*, 5523.

- (19) (a) Tomasi, J.; Persico, M. *Chem. Rev.* **1994**, *94*, 2027. (b) Takano, Y.; Houk, K. N. *J. Chem. Theory Comput.* **2005**, *1*, 70.
- (20) For discussions of DFT calculations on pericyclic reactions, see: (a) Guner, V. A.; Khuong, K. S.; Houk, K. N.; Chuma, A.; Pulay, P. *J. Phys. Chem. A* **2004**, *108*, 2959. (b) Guner, V.; Khuong, K. S.; Leach, A. G.; Lee, P. S.; Bartberger, M. D.; Houk, K. N. *J. Phys. Chem. A* **2003**, *107*, 11445.
- (21) For recent applications of DFT calculations on mechanistic studies of organic and organometallic reactions, see: (a) Niu, S.; Hall, M. B. *Chem. Rev.* **2000**, *100*, 353. (b) O'Neil, L. L.; Wiest, O. *J. Org. Chem.* **2006**, *71*, 8926. (c) Zhong, G.; Chan, B.; Radom, L. *J. Am. Chem. Soc.* **2007**, *129*, 924. (d) Gutta, P.; Tantillo, D. J. *J. Am. Chem. Soc.* **2006**, *128*, 6172. (e) Nova, A.; Ujaque, G.; Maseras, F.; Lledos, A.; Espinet, P. *J. Am. Chem. Soc.* **2006**, *128*, 14571.
- (22) For recent applications of DFT to study diradical species, see: (a) Yu, Z.-X.; Caramella, P.; Houk, K. N. *J. Am. Chem. Soc.* **2003**, *125*, 15420. (b) Jabbari, A.; Houk, K. N. *Org. Lett.* **2006**, *8*, 5975. (c) Bethke, S.; Hrovat, D. A.; Borden, W. T.; Gleiter, R. *J. Org. Chem.* **2004**, *69*, 3294. (d) Hoenigman, R. L.; Kato, S.; Bierbaum, V. M.; Borden, W. T. *J. Am. Chem. Soc.* **2005**, *127*, 17772. (e) Nummela, J. A.; Carpenter, B. K. *J. Am. Chem. Soc.* **2002**, *124*, 8512.

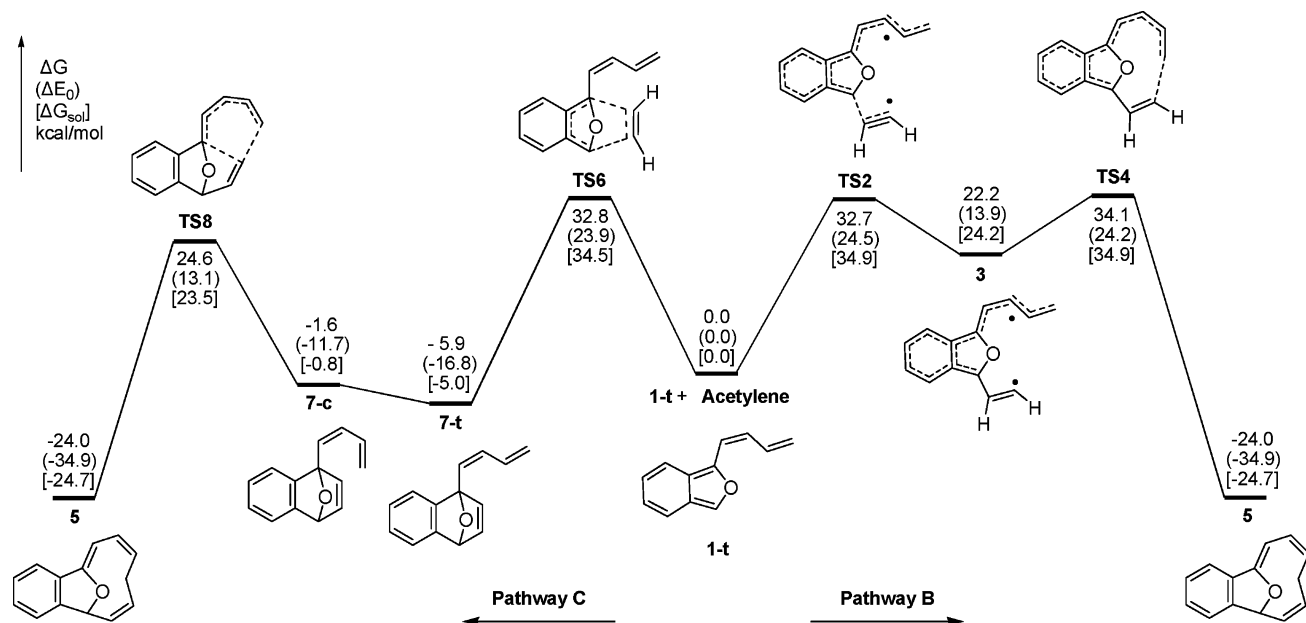
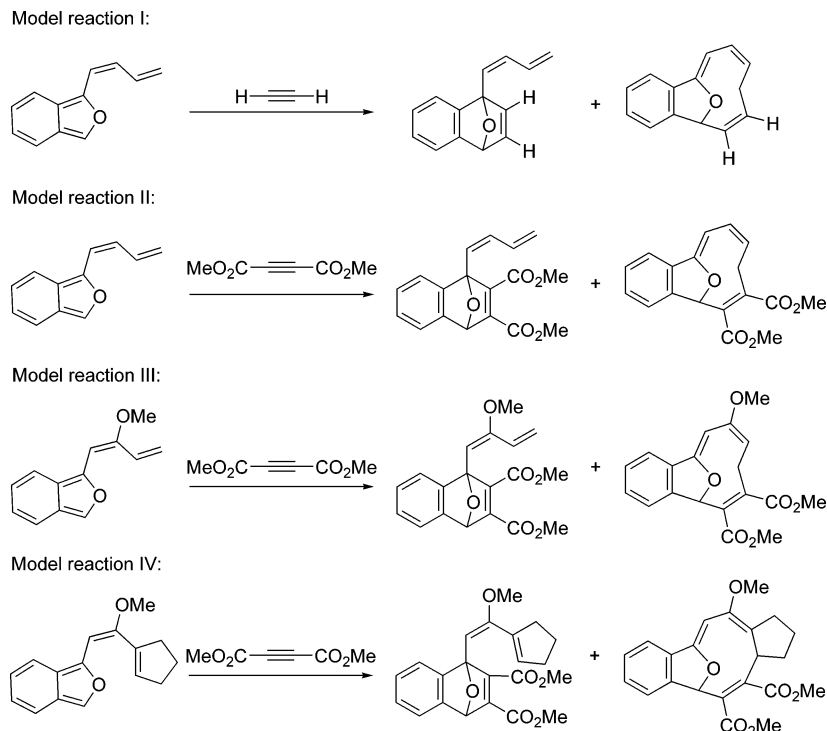


Figure 1. Computed energy surfaces of pathways B and C of model reaction I between tetraene **1** and acetylene at the (U)B3LYP/6-31+G(d) level.

Scheme 4. The Four Model Reactions Studied by DFT Calculations



reaction I. The DFT optimized transition states involved in both pathways are given in Figure 2 (the discussed atom numbering is also given in this Figure).

The parent tetraene of dienylibenzofuran **1** has two conformers, **1-t** and **1-c** (t and c denote the s-trans and s-cis configurations of the butadienyl moiety in **1**). Calculations indicate that **1-t** is the ground-state conformer and is more stable than **1-c** by 5.4 kcal/mol in terms of free energy. However, conformer **1-c**, in which the terminal carbons C1 and C8 are geometrically close with a distance of 4.25 Å, is expected to be the reacting conformer for a concerted [8+2] cycloaddition through pathway A. We can locate a concerted [8+2] transition structure between **1-c** and acetylene at the B3LYP/6-31G(d)

level of theory and at the Hartree–Fock theory with various basis sets (see Supporting Information for this concerted [8+2] TS). However, at the B3LYP/6-31+G(d) level, such a concerted [8+2] transition state could not be located. Using other DFT methods (such as BP86 and MPW1K) and the MP2 method, such a concerted [8+2] transition structure could not be obtained either. The failure of locating a concerted [8+2] cycloaddition at the B3LYP/6-31+G(d) level and others could be due to the possibility that such a concerted process is energetically disfavored as compared to the stepwise diradical pathway B. Calculations indicated that the concerted [8+2] transition structure at the B3LYP/6-31+G(d)/B3LYP/6-31G(d) level is higher in energy than diradical C–C bond formation transition

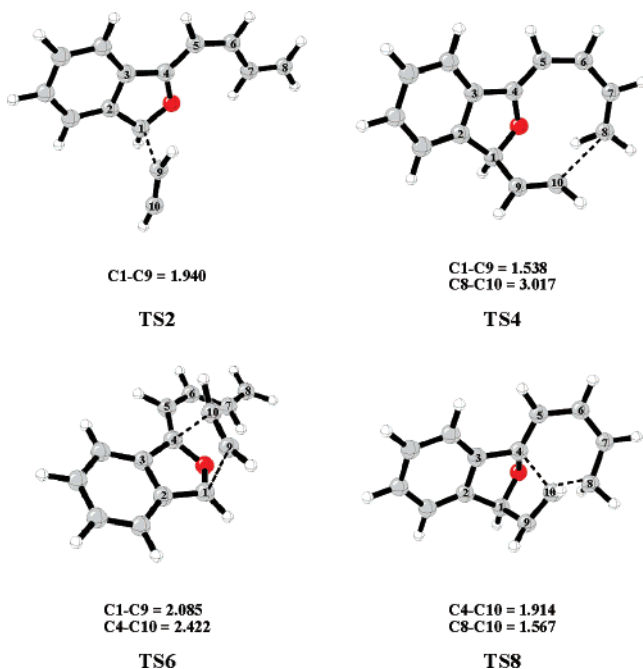


Figure 2. Computed geometries of transition states involved in pathways B and C of model reaction I. Distances are in angstroms.

structure **TS2** (see below) of pathway B by 7.8 kcal/mol, indicating that concerted [8+2] is inherently disfavored as compared to pathway B of the parent [8+2] cycloaddition.

The first step in pathway B is the formation of a single C–C bond between C1 and C9 via a diradical transition structure **TS2**, in which the forming C–C bond distance is 1.94 Å. The alkyne moiety in this transition structure is pointing away from the benzofuran ring with the dihedral angle of C10–C9–C1–C2 of 112.9°. The computed $\langle S^2 \rangle$ for **TS2** is 0.33. This step requires an activation free energy of 32.7 kcal/mol and an activation energy of 24.5 kcal/mol. The formed diradical intermediate **3** with a computed $\langle S^2 \rangle$ of 1.05 is higher in energy than the reactants by 22.2 kcal/mol. The second step is a one-step ring-closure reaction via **TS4**, which is higher in free energy than the diradical intermediate **3** by 11.9 kcal/mol and has a computed $\langle S^2 \rangle$ of 0.81. Formation of the [8+2] cycloadduct **5** is exergonic by 24.0 kcal/mol. Although **TS2** and **TS4** are close in terms of electronic energy (24.5 vs 24.2 kcal/mol), the latter is higher than the former by 1.4 kcal/mol in terms of free energy, suggesting that in gas phase, the rate-determining transition state in the stepwise diradical pathway B is the ring-closure **TS4** and the overall activation free energy of pathway B is 34.1 kcal/mol.

Pathway C of model reaction I starts from a Diels–Alder reaction between **1-t** and acetylene via **TS6**. Transition structure **TS6** has almost the same free energy as that of **TS2** of pathway B. The [4+2] transition structure **TS6** is concerted but asynchronous with the two forming C–C bonds of 2.09 (C1–C9) and 2.42 Å (C4–C10), respectively. IRC calculations indicate that **TS6** leads to formation of **7** without involvement of a zwitterionic intermediate. The [4+2] cycloadduct **7** also has two conformers, **7-c** and **7-t**, with the former being higher in energy than the latter by 4.3 kcal/mol. The [4+2] step in pathway C requires an activation free energy and an activation energy of 32.8 and 23.9 kcal/mol, respectively, and is exergonic by 5.9 kcal/mol. The [4+2] cycloaddition step in pathway C can be

cataloged as a normal-electron demand Diels–Alder cycloaddition because the energy gap of HOMO₁–LUMO_{acetylene} is smaller than the energy gap of HOMO_{acetylene}–LUMO₁ (see Figure 3).^{23,24} In addition, the charge transfer from **1** to acetylene in **TS6** is 0.014 electrons in terms of Mulliken charge, further demonstrating the character of normal electron demand Diels–Alder reaction for **TS6**. The FMO of **1-c** is also given in Figure 3. We can understand why a concerted [8+2] is not favored in view of the fact that the orbital coefficient of C8 is smaller than both C1 and C4 in the HOMO of **1-c**, suggesting that C8 is not reactive in cycloaddition as compared to C1 and C4 in **1**. This is also consistent with the high reactivity of the furan moieties in isobenzofurans.²⁵

The parent [8+2] reaction of pathway C could stop at the Diels–Alder reaction if the ensuing [1,5]-vinyl shift is difficult. Calculations show that the [1,5]-vinyl shift in pathway C starts from an s-trans to s-cis interconversion step, transforming **7-t** to **7-c**, which is the reacting conformer for [1,5]-vinyl shift. The energy required to undergo cis/trans isomerization is negligible when compared to those required for the [4+2] and the [1,5]-vinyl shift.²⁶

We could locate a concerted, closed-shell singlet [1,5]-vinyl shift transition structure using the restricted B3LYP/6-31+G(d) method. However, it was found that a concerted open-shell singlet diradical transition structure **TS8** located at the UB3LYP/6-31+G(d) level is more stable by 3.5 kcal/mol than the closed-shell singlet vinyl shift transition structure.^{16,17} The diradical **TS8** with a computed $\langle S^2 \rangle$ of 0.51 has a long breaking bond (1.91 Å) and a short forming C–C bond (1.57 Å). This is a very late transition state because the forming bond is almost formed. The overall process from **7-t** → **7-c** → **5** requires an activation free energy of 30.5 kcal/mol.

The rate-determining step in pathway C is the [4+2] cycloaddition, indicating that the activation free energy required for pathway C is 32.8 kcal/mol. Comparing this to the activation free energy of 34.1 kcal/mol required for pathway B, we can conclude pathway B is disfavored by 1.3 kcal/mol in terms of activation free energy.

The above theoretical analysis revealed that model reaction I between **1-t** and acetylene has two competitive pathways, B and C. The stepwise diradical pathway B can lead to the formation of a [8+2] cycloadduct, whereas stepwise [4+2]/[1,5]-vinyl shift pathway C can lead to the formation of a [4+2] cycloadduct, which can then isomerize to the [8+2] cycloadduct.

- (23) FMO theory: (a) Fleming, I. *Frontier Orbitals and Organic Chemical Reactions*; Wiley & Sons: New York, 1996. (b) Dewar, M. J. S. *The Molecular Orbital Theory for Organic Chemistry*; McGraw-Hill: New York, 1969. (c) Zimmerman, H. E. *Acc. Chem. Res.* **1971**, *4*, 272. (d) Sustmann, R. *Tetrahedron Lett.* **1971**, *12*, 2721. (e) Sustmann, R.; Schubert, R. *Angew. Chem., Int. Ed. Engl.* **1972**, *11*, 840. (f) Sustmann, R. *Pure Appl. Chem.* **1974**, *40*, 569. (g) Houk, K. N. *Acc. Chem. Res.* **1975**, *8*, 361. (h) Houk, K. N. *J. Am. Chem. Soc.* **1973**, *95*, 4092.
- (24) For recent reviews and researches on normal and inverse electron-demanded Diels–Alder reactions, see: (a) ref 23d. (b) Sauer, J.; Sustmann, R. *Angew. Chem., Int. Ed. Engl.* **1980**, *19*, 779. (c) Yu, Z.-X.; Dang, Q.; Wu, Y.-D. *J. Org. Chem.* **2001**, *66*, 6029. (d) Yu, Z.-X.; Dang, Q.; Wu, Y.-D. *J. Org. Chem.* **2005**, *70*, 998. (e) Dai, M.; Sarlah, D.; Yu, M.; Danishefsky, S. J.; Jones, G. O.; Houk, K. N. *J. Am. Chem. Soc.* **2007**, *129*, 645. (f) Gomez-Bengoa, E.; Helm, M. D.; Plant, A.; Harrity, J. P. A. *J. Am. Chem. Soc.* **2007**, *129*, 2691.
- (25) For references of isobenzofurans, see: (a) Wiersum, U. E.; Mijs, W. J. *J. Chem. Soc., Chem. Commun.* **1972**, 347. (b) Berson, J. A. *J. Am. Chem. Soc.* **1953**, *75*, 1240. (c) Rio, G.; Scholl, M.-J. *J. Chem. Soc., Chem. Commun.* **1975**, 474. (d) Faragher, R.; Gilchrist, T. L. *J. Chem. Soc., Perkin Trans. 1* **1976**, 336. (e) Tobia, D.; Rickborn, B. *J. Org. Chem.* **1987**, *52*, 2611.
- (26) For a study of the cis–trans interconversion of butadiene, see: Squillacote, M. E.; Liang, F. *J. Org. Chem.* **2005**, *70*, 6564.

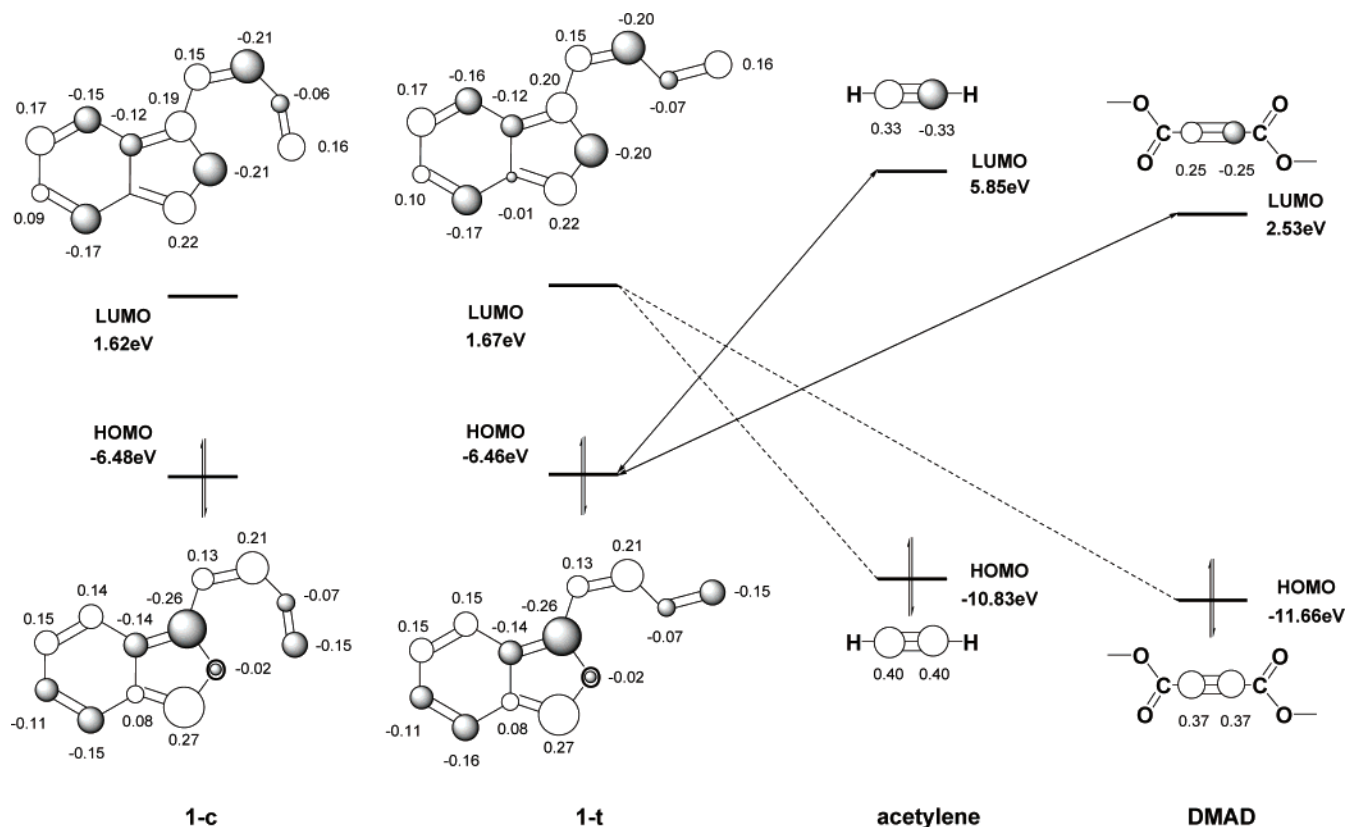


Figure 3. Frontier molecular orbitals of **1**, acetylene, and DMAD. The orbital coefficients are referred to the 2p part of each heavy atom. Atom numbering is referred to that in Figure 2.

The dominant pathway for the [8+2] cycloaddition of model reaction I is pathway C because it is preferred over pathway B by 1.3 kcal/mol in terms of activation free energy in gas phase.

It is interesting to point out that the formation of the [8+2] cycloadduct is thermodynamically preferred over the formation of the [4+2] cycloadduct because the [8+2] cycloadduct is more stable than the [4+2] cycloadduct by 18.1 kcal/mol. This thermodynamic preference of [8+2] cycloadduct is the driving force for the [1,5]-vinyl shift. The lower energy of [8+2] cycloadduct as compared to the [4+2] cycloadduct can be attributed to less ring strain and more conjugation in the [8+2] cycloadduct relative to the [4+2] cycloadduct.

As compared to the gas-phase energy surfaces of model reaction I, in solution, the stepwise diradical pathway B and the [4+2] step of pathway C are disfavored by 2.2 and 1.7 kcal/mol, respectively (see Figure 1). In contrast, the vinyl shift step in solution is easier by 2.0 kcal/mol with respect to that rearrangement in gas phase (28.5 vs 30.5 kcal/mol). Nevertheless, in solution, pathway C is still favored over pathway B for model reaction I.

3.2. Theoretical Study of Model Reaction II and the Experimental Test of the Theoretical Prediction. We now turn our attention to model reaction II between **1** and DMAD to investigate its reaction mechanism and energetic differences with respect to those in model reaction I. Figure 4 shows the computed energy surfaces of pathways B and C. The optimized geometries of the transition states involved are given in Figure 5. Calculations show that pathway A is not feasible, similar to model reaction I. All attempts to use other DFT functionals in conjunction with either 6-31G(d) or 6-31+G(d) basis set to

locate a concerted [8+2] transition structure only led to locating a [4+2] cycloaddition transition structure, further demonstrating that a direct concerted [8+2] cycloaddition is disfavored as compared to a [4+2] cycloaddition.

In contrast to model reaction I, where pathway B is a stepwise diradical pathway, pathway B here is through a stepwise zwitterionic route. The first step of pathway B is the formation of a zwitterionic intermediate **10** via transition structure **TS9**, which has the forming bond distance of C1–C9 of 2.06 Å. In **TS9**, the C9 atom must point away from the furan ring with the dihedral angle of C10–C9–C1–C4 of 179.1°, otherwise, only concerted [4+2] transition structure **TS13** of pathway C, where both C9 and C10 are above the furan moiety of **1**, can be located. The formation of **10** requires an activation free energy of 33.5 kcal/mol and an activation energy of 21.4 kcal/mol in gas phase. The following ring-closure step to form the [8+2] cycloadduct is very easy and occurs with an activation free energy of 2.9 kcal/mol. All attempts to locate a ring-closure transition structure for the formation of a [4+2] cycloadduct **14-t** from intermediate **10** (instead of a [8+2] cycloadduct **12**) were unsuccessful, suggesting **14-t** is formed only through a Diels–Alder reaction (see discussions below). As compared to model reaction I, pathway B of model reaction II has the C1–C9 bond formation as the rate-determining step with an activation free energy of 33.5 kcal/mol, which is 0.6 kcal/mol lower than the stepwise diradical pathway B of model reaction I. However, pathway B of model reaction II is still disfavored as compared to pathway C, which has an activation free energy of 30.5 kcal/mol (see below). This suggests that if the [8+2] cycloadduct could be obtained in model reaction II, the reaction would take place through pathway C.

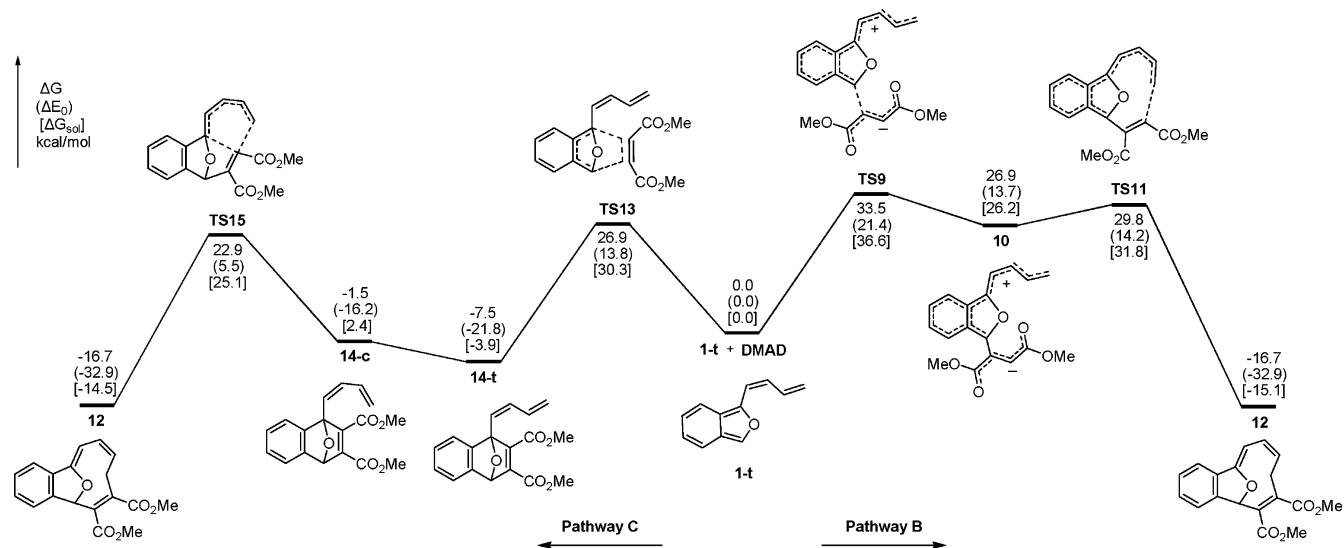


Figure 4. Potential energy surface of pathways B and C of model reaction II between **1** and DMAD computed at the (U)B3LYP/6-31+G(d) level.

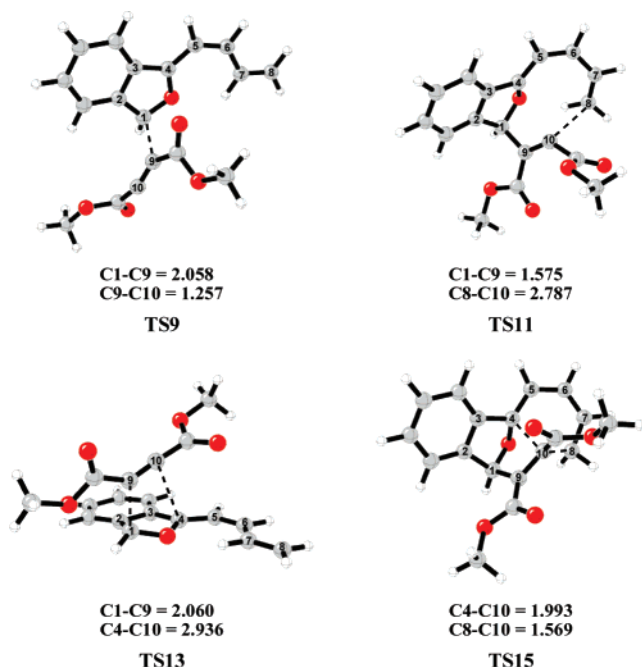


Figure 5. Computed geometries of transition states involved in pathway C of model reaction II. Distances are in angstroms.

Pathway C of model reaction II starts from an exergonic (by 7.5 kcal/mol) [4+2] cycloaddition with an activation free energy of 26.9 kcal/mol and an activation energy of 13.8 kcal/mol via **TS13**. As compared to the Diels–Alder reaction step in pathway C of model reaction I, the activation free energy of the [4+2] step in model reaction II is lower by 5.9 kcal/mol. This can be well rationalized by FMO theory because the LUMO of DMAD is lower than that of acetylene by 3.32 eV (Figure 3). In **TS13**, the charge transfer from **1-t** to DMAD is 0.217 electrons in terms of Mulliken charge. Transition structure **TS13** is more asynchronous because the forming C–C bond is 2.06 Å while the other forming C–C bond is hardly formed at all with a distance of 2.94 Å. This [4+2] process can be regarded as a two-stage process because the formation of one bond is more advanced than the other without involvement of a zwitterionic intermediate.²⁷

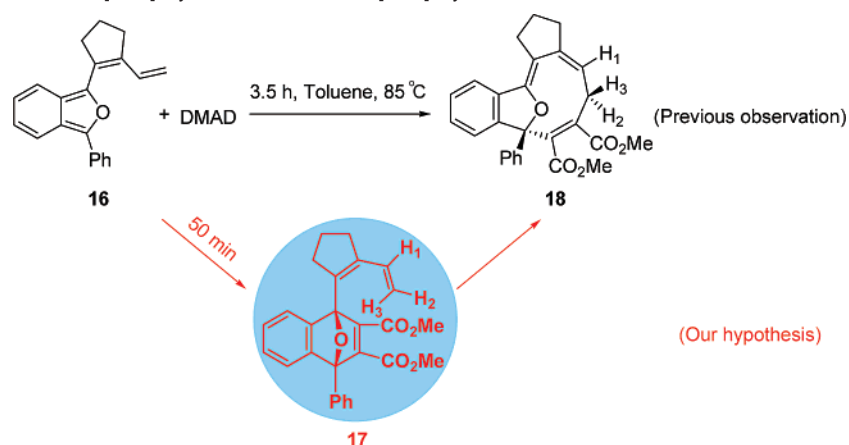
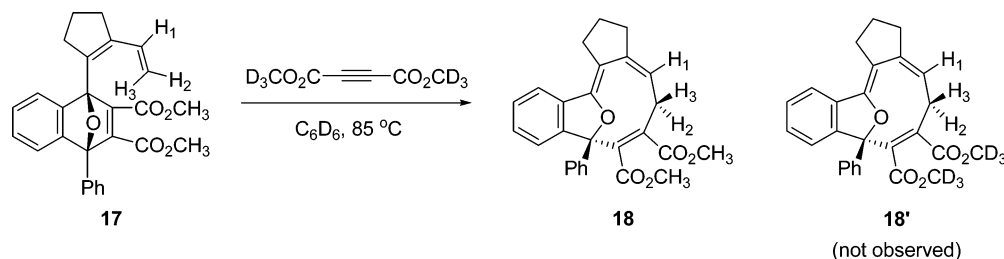
Subsequent s-trans to s-cis interconversion from **14-t** to **14-c** and a vinyl shift process takes place with an activation free energy of 30.4 kcal/mol via **TS15**. This isomerization step is exergonic by 9.2 kcal/mol. The vinyl shift transition structure in model reaction II is also a very late transition structure with distances of 1.99 and 1.57 Å for the breaking and forming bonds, respectively.

In solution, pathway B has an activation free energy of 36.6 kcal/mol, 3.1 kcal/mol higher than that in gas phase. In solution, the [4+2] step of pathway C also becomes more difficult by 3.4 kcal/mol in terms of activation free energy. Similar to model reaction I, the [1,5]-vinyl shift in solution is easier by 1.4 kcal/mol as compared to that in gas phase. Figure 3 shows that even in solution, pathway C is preferred over pathway B.

If model reaction II could occur via pathway C, the [1,5]-vinyl shift would be the rate-determining step. This is due to the fact that the activation free energy of the [1,5]-vinyl shift is higher by 3.5 kcal/mol than that of the [4+2] cycloaddition (30.4 vs 26.9 kcal/mol) in gas phase. In solution, the vinyl shift requires an activation free energy of 29.0 kcal/mol, 1.3 kcal/mol lower than the [4+2] step with an activation energy of 30.3 kcal/mol. It is well known that computationally calculated activation free energies for bi- or trimolecular reactions in solution are overestimated by a few kcal/mol.²⁸ In this regard, in solution, the [1,5]-vinyl shift is still more difficult than the bimolecular [4+2] process. Because the formation of [4+2] cycloadduct is exergonic and the following [1,5]-vinyl shift requires higher activation free energy, we hypothesized that model reaction II could stop at the formation of the [4+2] cycloadduct, if the reaction temperature is decreased or the reaction time is shortened. If we could obtain the [4+2]

(27) (a) Dewar, M. J. S.; Olivella, S.; Stewart, J. J. P. *J. Am. Chem. Soc.* **1986**, *108*, 5771–5779. (b) Domingo, L. R.; Picher, M. T.; Arroyo, P.; Sáez, J. A. *J. Org. Chem.* **2006**, *71*, 9319.

(28) For discussions of entropy overestimation in bimolecular reactions in aqueous solution, see: (a) Strajbl, M.; Sham, Y. Y.; Villa, J.; Chu, Z.-T.; Warshel, A. *J. Phys. Chem. B* **2000**, *104*, 4578. (b) Hermans, J.; Wang, L. *J. Am. Chem. Soc.* **1997**, *119*, 2707. (c) Amzel, L. M. *Proteins* **1997**, *28*, 144. (d) Yu, Z.-X.; Houk, K. N. *J. Am. Chem. Soc.* **2003**, *125*, 13825. (e) Xia, Y.; Liang, Y.; Chen, Y.; Wang, M.; Jiao, L.; Huang, F.; Liu, S.; Li, Y.; Yu, Z.-X. *J. Am. Chem. Soc.* **2007**, *129*, 3470.

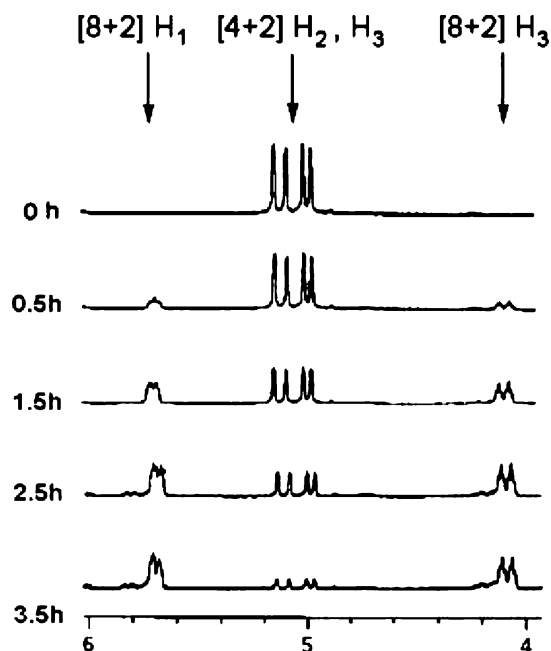
Scheme 5. Experiments To Isolate [4+2] Cycloadduct and Test [4+2] Cycloadduct's Isomerization**Scheme 6.** Crossover Experiment

cycloadduct, we then would be able to monitor the [1,5]-vinyl shift process experimentally to support our computational prediction.

To test our hypothesis, we focused on the reaction between **16** and DMAD shown in Scheme 5. In the previous report,^{7a} the reaction was conducted in toluene at 85 °C for 3.5 h and only [8+2] cycloadduct **18** was obtained. We speculated that by running the [8+2] reaction between **16** and DMAD at lower temperature or heating this reaction in a shorter time, we could isolate the [4+2] cycloadduct **17**. Monitoring the isomerization of **17** to **18** would then give direct evidence to either support or disprove our theoretical prediction in Figure 4. Therefore, we followed the previous procedure to synthesize substrate **16** and then ran the reaction between **16** and DMAD in toluene at 85 °C. To our excitement, after a 50-min reaction period, a mixture of [4+2] and [8+2] cycloadducts **17** and **18** in a ratio of 3.3:1 was obtained with a total yield of 59% (Scheme 5).

Figure 6 shows how **17** gradually isomerized to **18** upon heating at 80 °C in deuterated benzene by ¹H NMR spectroscopy. Formation of **18** became obvious after 30 min of heating **17**, when the ratio of **18/17** was 1:5. The ratio of **18/17** increased after further heating. After about 3.5 h, the major substance in the NMR tube was **18** with the ratio of **18/17** of 10:1. This experiment suggests that **17** can be transformed to **18**, but cannot guarantee that this transformation occurs via an intramolecular [1,5]-vinyl shift. This is due to the possibility that the generation of **18** from **17** could arguably take place through a two-step process, starting from the retro-Diels–Alder reaction of **17** to generate dienylobenzofuran **16** and DMAD, which then react with one another through a concerted or stepwise [8+2] cycloaddition process to give the [8+2] cycloadduct **18**. To rule out this possibility, it is necessary to prove that the isomerization of **17** to **18** is an intramolecular process instead of an intermolecular process.

Isomerization of **17** in the presence of 10 equiv of DMAD-*d*₆ ($CD_3O_2C-C\equiv C-CO_2CD_3$) at 85 °C in deuterated benzene was examined (Scheme 6). After this reaction system was heated for 8 h, only the non-deuterated **18** was observed without any incorporation of deuterated DMAD. This assignment was based on the ratio of hydrogens on ester group of **18** as compared to the other hydrogens of **18** according to the signals in the ¹H NMR spectrum. Experimental observation of no formation of any crossover product **18'** clearly demonstrated that the isomer-

**Figure 6.** Monitoring the vinyl shift of **17** to **18** by ¹H NMR in C_6D_6 . The atom labeling is given in Scheme 5.

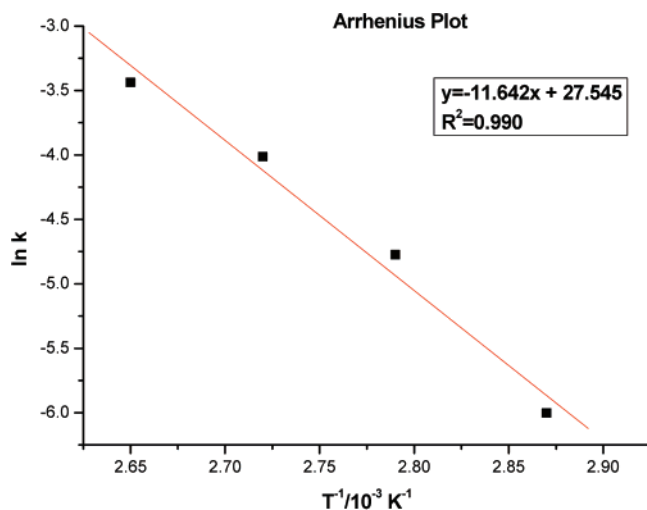


Figure 7. Arrhenius plot for the [1,5]-vinyl shift of **17** to **18**.

ization of **17** to **18** takes place in an intramolecular fashion and occurs via a [1,5]-vinyl shift process.

The above theoretical and experimental evidence strongly supports that the formation of [8+2] cycloadduct in this case is through a stepwise mechanism via [4+2]/[1,5]-vinyl shift process. The discovery of this newly proposed mechanism suggests that 10-membered ring compounds could be synthesized via such a ring enlargement strategy⁹ to complement the one-pot [8+2] strategy highlighted in Scheme 2.

Finally, we wanted to test the accuracy of the DFT method used in this study. The best way to do this is to compare the DFT computed activation barrier with the experimentally measured one for the isomerization of **17** to **18**. The kinetics of this isomerization process has been quantitatively studied by means of ¹H NMR through heating the [4+2] product **17** in toluene-*d*₈ (details are given in the Supporting Information). The kinetics of the [1,5]-vinyl shift process were investigated at four different temperatures, 75.0, 85.0, 95.0, and 105.0 °C, respectively. Activation parameters $k = 9.2 \times 10^{11} \exp(-23.0/RT) \text{ min}^{-1}$ were obtained from the Arrhenius plot (Figure 7). From the Arrhenius plot, the activation energy of the [1,5]-vinyl shift is estimated to be $23.0 \pm 2.3 \text{ kcal/mol}$. The measured ΔG^\ddagger , ΔH^\ddagger , and ΔS^\ddagger values of this isomerization are 24.2 kcal/mol, 22.3 kcal/mol, and $-6.2 \text{ cal/(mol}\cdot\text{K)}$, respectively. With this experimentally measured activation energy in hand, we computed the [1,5]-vinyl shift process from **19** to **21** depicted in Figure 8. This system is similar to the experimental one (**17** to **18**) except the phenyl group in **17** is substituted by a hydrogen atom. To our delight, the computed activation free energy from **19** to **21** in benzene is 24.0 kcal/mol, which is in great agreement with the experimental activation energy, suggesting that DFT is quite good in predicting the activation parameters for the present [8+2] reaction (Figure 8). The computed ΔH^\ddagger (21.8 kcal/mol) and ΔS^\ddagger ($-11.7 \text{ cal/(mol}\cdot\text{K)}$) values in gas phase are also close to those measured experimentally in toluene.

3.3. Model Reactions III and IV: Methoxy Group Is Critical To Switch Pathway C to Pathway B. In the original report of the [8+2] cycloaddition reactions,^{7a} it was observed that the reactions of **22a–d** with DMAD can give both [4+2] cycloadducts **23a–d** and [8+2] cycloadducts **24a–d**, and the ratio of **23a–d**/**24a–d** depends on the substituents in **22a–d** (Scheme 7). To test whether these [8+2] reactions occur via

pathway C, a simple experimental test can determine whether compounds **24a–d** were formed via [1,5]-vinyl shift isomerizations from compounds **23a–d**. Therefore, we synthesized and isolated four [4+2] cycloadducts **23a–d** according to the previous procedures.^{7a} To our surprise, heating these [4+2] cycloadducts **23a–d** in dioxane at 85 °C did not lead to formation of **24a–d**. Heating compounds **23a–d** longer or under higher temperatures (in toluene at 110 °C) only resulted in decomposition. These experiments demonstrated that [1,5]-vinyl shifts are difficult for **23a–d**, and the formation of **24a–d** is not through pathway C.

Why is there a mechanistic difference for the [8+2] reactions of **22a–d** versus **16** toward DMAD? After comparing the structural differences between **22a–d** and **16**, we hypothesized that the different mechanisms for the formation of [8+2] cycloadducts might be attributed to the methoxy group in **22a–d**. In model reaction II, pathway B is disfavored with respect to pathway C. However, we reasoned that in the cases of **22a–d**, the methoxy group in the diene moiety could stabilize the zwitterionic transition structures in pathway B to a greater extent than the transition structures of pathway C, making pathway B competitive with pathway C. In this scenario, the final [8+2] cycloadducts could result from either pathway B or C. However, if the [1,5]-vinyl shift is difficult and pathway C would stop at the [4+2] step, the final products would consist of both [8+2] cycloadducts (via pathway B) and [4+2] cycloadducts (via the Diels–Alder reaction of pathway C). To better explain the experimental results in Scheme 7, we studied model reactions III and IV to investigate the influence of the methoxy group on the reaction outcome. We will first discuss model reaction III and the reaction of **22a** and DMAD. We will then discuss model reaction IV and the reactions of **22b–d** and DMAD to explore whether the cyclic ring in the terminal alkene of the tetraenes has additional influence on the reaction mechanism. The computed energy surfaces for pathways B and C of model reaction III are given in Figure 9.

Pathways B and C of model reaction III are similar to those of model reaction II, and the geometries of the stationary points in these pathways will not be discussed in detail. One major difference of pathway B in model reactions II and III is the activation free energies of the first C–C bond formation step, which is 33.5 kcal/mol for model reaction II and 25.1 kcal/mol for model reaction III, confirming our hypothesis about the stabilizing influence of the methoxy group. Formation of intermediate **26** in model reaction III is less endergonic than the formation of **10** in model reaction II by 6.6 kcal/mol, further confirming that the methoxy group is very effective at stabilizing the zwitterionic species. The ring closure step for model reaction III is also more facile via **TS27** with an activation free energy of 3.2 kcal/mol.

In pathway C, the [4+2] cycloaddition between the furan moiety of **1-OMe** and DMAD is easier than the corresponding cycloaddition between furan moiety of **1** and DMAD (22.8 vs 26.9 kcal/mol in terms of activation free energy). The higher [4+2] reactivity of **1-OMe** as compared to **1** is due to the higher HOMO energy of the methoxy-containing tetraenes (-6.39 vs -6.46 eV) based on FMO theory. The activation free energy of the [1,5]-vinyl shift of **30-t** to **28** in model reaction III is lower by 3.0 kcal/mol than that of the vinyl shift converting **14-t** to **12** in model reaction II (27.4 vs 30.4 kcal/mol). The

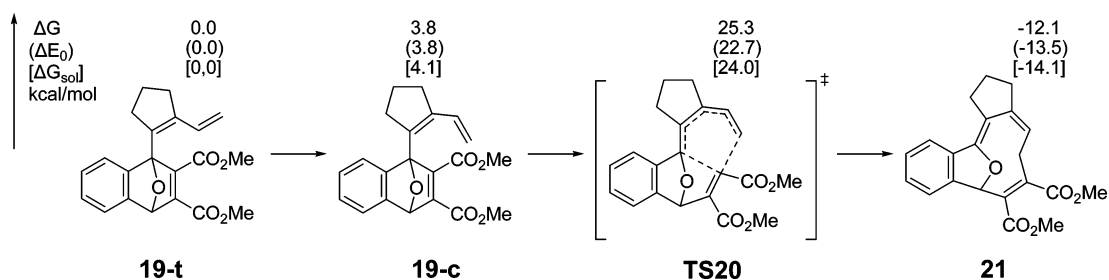
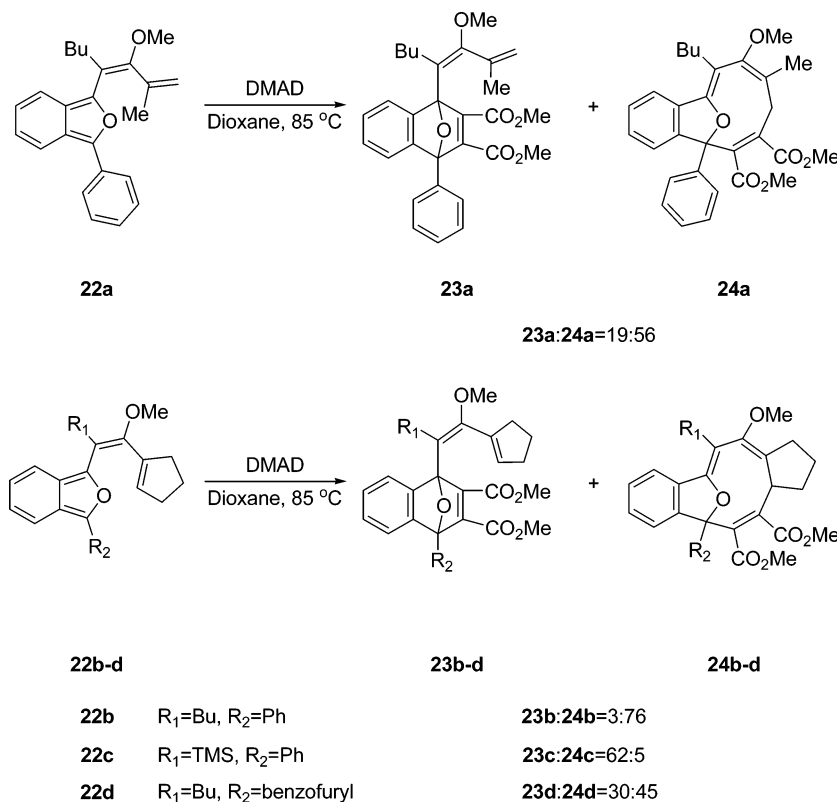


Figure 8. Relative energies for the isomerization of **19** to **21** computed at the (U)B3LYP/6-31+G(d) level.

Scheme 7. Previously Reported [8+2] Reactions



easier [1,5]-vinyl shift of **30-t** to **28** is due to additional stabilization of the diradical isomerization transition state by the methoxy group because radical species are usually stabilized by heteroatoms.²⁹ Pathway C of model reaction III would stop at the [4+2] cycloaddition because the rate-determining step is the [1,5]-vinyl shift.

In solution, pathway B has an activation free energy of 28.4 kcal/mol, 3.3 kcal/mol higher than that in gas phase. In solution, the [4+2] step of pathway C becomes also difficult by 4.2 kcal/mol in terms of activation free energy. Similar to model reactions I and II, the [1,5]-vinyl shift in solution is easier by 1.8 kcal/mol as compared to that in gas phase. Figure 9 shows that even in solution, pathway C is preferred over pathway B.

How can the experimental observation that a reaction similar to model reaction III stops at the [4+2] cycloaddition step be rationalized? Even though the methoxy group can reduce the activation free energy of the [1,5]-vinyl shift by 3 kcal/mol both in gas phase (27.4 vs 30.4 kcal/mol) and in solution (25.6 vs 29.0 kcal/mol), this isomerization of **30-t** to **28** of model reaction

III in solution is still about 1.4 kcal/mol higher than that of the isomerization of **17** to **18**, which is experimentally observed and has a measured activation energy of 24.2 kcal/mol. The model isomerization of **30-t** to **28** is very similar to the isomerization of **23a** to **24a**, suggesting that the isomerization of **23a** to **24a** also requires an activation energy close to 25.6 kcal/mol. Therefore, the activation free energy of **23a** to **24a** in solution is estimated to be about 1.4 kcal/mol higher than that of the isomerization of **17** to **18**. The isomerization of **17** to **18** can finish at 85 °C in 3.5 h; however, the isomerization of **23a** to **24a** should take longer or at higher temperature. Heating **23a** to a higher temperature causes decomposition, which may occur through pathways with activation energies lower than [1,5]-vinyl shift, to become competitive with isomerization. This is the reason why [1,5]-vinyl shift does not happen for **23a**.

Now let us focus on explaining why the reactions between **22a** and DMAD gave both [4+2] and [8+2] cycloadducts. Model reaction III shows that pathway B can give an [8+2] cycloadduct and pathway C can give a [4+2] cycloadduct, which does not isomerize to the [8+2] cycloadduct. The ratio of [8+2]/

(29) For discussions of stabilization of radicals and diradicals, see: (a) Baldwin, J. E. *Chem. Rev.* **2003**, *103*, 1197. (b) Togo, H. *Advanced Free Radical Reactions for Organic Synthesis*; Elsevier Press: Amsterdam, 2004.

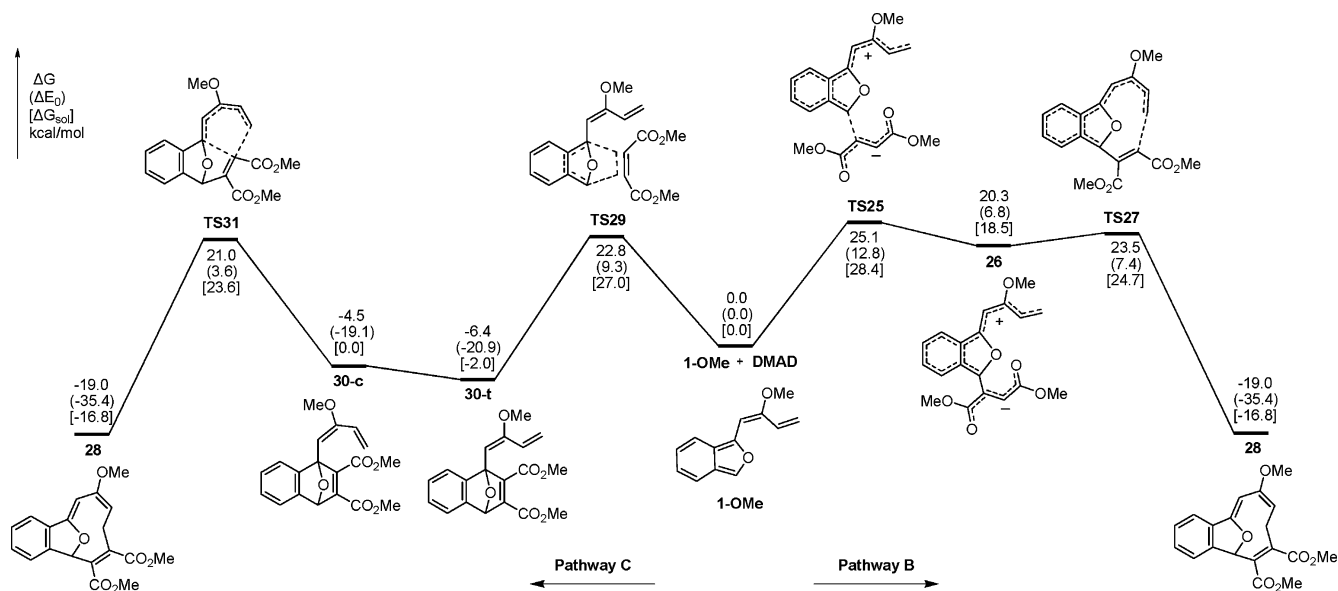


Figure 9. Potential energy surface of pathways B and C of model reaction III between 1-OMe and DMAD computed at the (U)B3LYP/6-31+G(d) level.

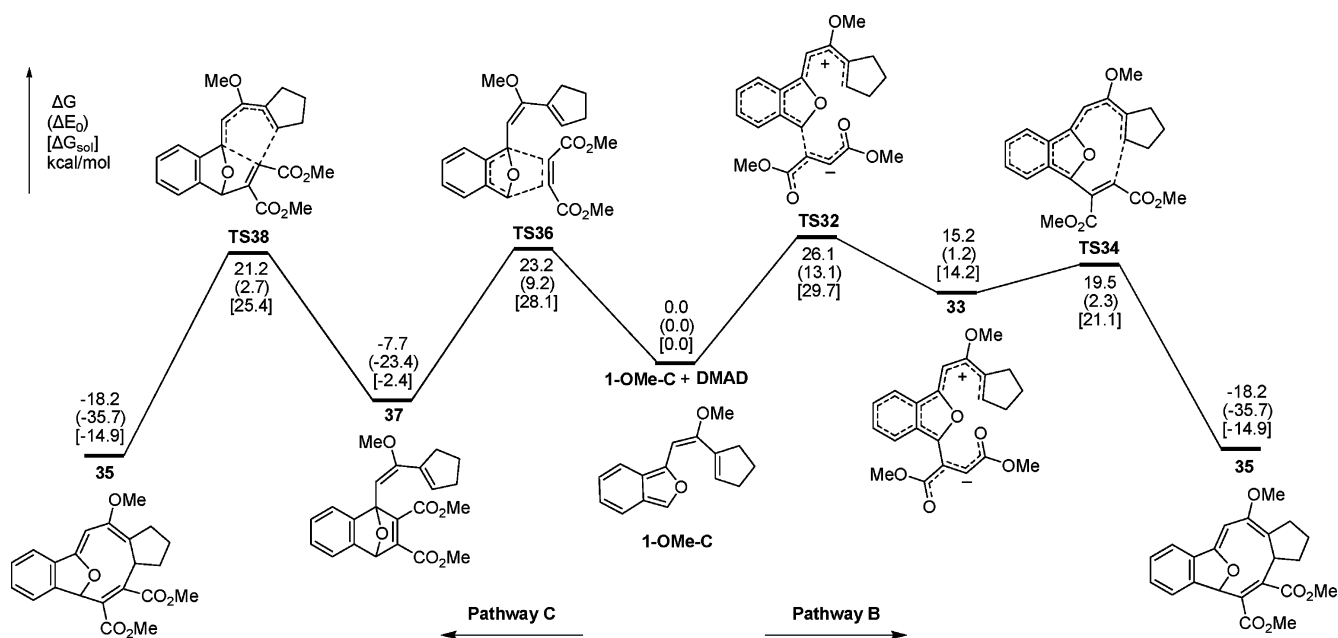


Figure 10. Potential energy surface of pathways B and C of the model reaction IV between 1-OMe-C and DMAD computed at the (U)B3LYP/6-31+G(d) level.

[4+2] would be determined by the relative activation free energies of pathways B and C. In gas phase, the formed products would be dominated by the [4+2] cycloadduct because pathway B to give [8+2] cycloadduct requires an activation free energy that is about 2.3 kcal/mol higher than the [4+2] transition state structure **TS29**. However, in solution, the percentage of [8+2] cycloadduct will increase because the zwitterionic **TS25** and intermediate **26** will be stabilized more significantly by the solvent interaction as compared to the [4+2] transition state. **TS25** has a dipole moment of 6.12 debye, while **TS29** has a dipole moment of 5.40 debye. Calculations show the preference of pathway C over pathway B is decreased to about 1.4–1.0 kcal/mol in benzene and other solvents such as dioxane, ether, THF, and methanol (see Supporting Information for details). These computed results suggest that both [4+2] and [8+2]

cycloadducts in a ratio ranging from 10:1 to 6:1 can be obtained. This computationally predicted ratio for model reaction III in solution is reasonably comparable to the experimental measured ratio of 1:3 for the reaction of **22a** with DMAD (Scheme 7). Because the experimental systems contain a phenyl substituent at the furan moiety that is not present in the computational models, the DFT computed [8+2]/[4+2] ratio will be slightly different from the experimentally measured one.

Most of the [8+2] reactions reported previously have a cyclic structure in the terminal alkenes of the tetraenes (see **22b–d**).^{7a} To investigate the influence of its presence on the [8+2] reactions, model reaction IV has also been computed. The energy surfaces of pathways B and C are given in Figure 10, and the computed geometries of stationary points involved are given in the Supporting Information.

Figure 10 shows that the mechanism of **1-OMe-C** is similar to that of model reaction III. Let us first discuss why [1,5]-vinyl shifts for **23b-d** occur with difficulty. The computed isomerization of **37** to **35** in solution requires an activation free energy of 27.8 kcal/mol, 2.2 kcal/mol higher than the isomerization of **30-t** to **28** in model reaction III. This suggests that isomerization of **37** to **35** is even more difficult than other competitive pathways of the [4+2] cycloadducts. Consequently, we could not observe a [1,5]-vinyl shift for **23b-d**, which has estimated activation free energies for isomerization of about 28.9 kcal/mol in gas phase and 27.8 kcal/mol in solution, similar to the rearrangement of **37** to **35** in Figure 10.

Therefore, model reaction IV will give both [4+2] cycloadduct **37** and [8+2] cycloadduct **35**. In gas phase, pathway C is favored by 2.9 kcal/mol, suggesting that the dominant product of model reaction IV is [4+2] cycloadduct **37** and that the [8+2] cycloadduct is almost negligible. However, the computed preference of **37** over **35** is reduced by around 1.5 kcal/mol in various solvents such as dioxane, benzene, methanol, ether, and THF. This predicts that the **37:35** ratio should be around 10:1. Although the predicted values do not indicate that the [8+2] cycloadduct should be major as was observed experimentally, the calculations do suggest that the formations of **37** and **35** are competitive processes. Because the calculations were conducted on systems where R^1 and $R^2 = H$, it is reasonable that subtle structural changes could alter the [8+2]/[4+2] ratio, as was observed experimentally. For example, it is likely that sterically different substituent groups (e.g., TMS vs *n*-butyl) would have very different solvation energies. Comparison of the energy surfaces of model reactions III and IV indicates that the cyclic substituents in the tetraenes do not significantly alter the reaction scenario. The only difference is the [1,5]-vinyl shift in model reaction IV is more difficult.

From the theoretical studies of model reactions III and IV, together with the isomerization experiments, we can conclude that in the [8+2] reactions involving tetraenes **22a-d** with a methoxy group in the dienyl moieties, [8+2] cycloadducts **24** are formed via pathway B, and [4+2] cycloadducts **23** are formed via direct [4+2] Diels–Alder cycloadditions. The [4+2] cycloadducts **23** have difficulty undergoing [1,5]-vinyl shifts due to the higher activation free energies of these processes than those of various unknown decomposition pathways.

4. Conclusions

In conclusion, a combined theoretical and experimental study of [8+2] cycloadditions of dienylisobenzofurans and DMAD showed that the concerted, one-step [8+2] cycloaddition is not

favored. The stepwise pathway B via formation of either a diradical or a zwitterionic intermediate followed by ring closure can occur for the [8+2] cycloadditions. However, this pathway is not favored as compared to pathway C, which starts from a concerted, asynchronous [4+2] reaction and a diradical [1,5]-vinyl shift. Experiments have been performed to confirm that one previously reported [8+2] cycloaddition occurs through pathway C. When an electron-donating group is present in the dienyl moieties of tetraenes, pathway B is still not favored in gas phase but can compete in solution because the zwitterionic transition state in pathway B can be stabilized much more significantly than the transition structures in pathway C. These two pathways can compete with one another to furnish both [8+2] and [4+2] cycloadducts. In several cases, the [1,5]-vinyl shifts are difficult for the [4+2] cycloadducts shown in Scheme 7. The confirmation of pathway C in this study suggests a new strategy could be used to synthesize 10-membered or larger ring compounds. The unveiling of the stepwise mechanism for the present [8+2] cycloaddition implies that, even though many [8+2] and other high order [*m+n*] cycloadditions for the synthesis of large ring systems follow the Woodward–Hoffmann orbital symmetry rules, these reactions could also adopt stepwise mechanisms because the long distance between the terminal atoms of the reactants does not allow a concerted mechanism. Further study of other [8+2] cycloadditions and application of vinyl shift for ring-enlargement reactions⁹ are underway.

Acknowledgment. Z.-X.Y. and his group are indebted for generous financial support from a new faculty grant from Peking University, the Natural Science Foundation of China (9800445, 0240203, and 20672005), and the Scientific Research Foundation for the Returned Overseas Chinese Scholars, State Education Ministry of China. J.W.H. thanks the SCORE Program of NIH. Z.-X.Y. also thanks Prof. K. N. Houk of the University of California at Los Angeles (UCLA) for his many insightful suggestions, support, and encouragement of this project, and the theoretical and synthetic organic chemistry group at PKU. Ms. J. R. Luft from UCLA is highly appreciated for her help in improving our writing of this paper.

Supporting Information Available: Computational and experimental details, the Cartesian coordinates, energies of all computed stationary points, characterization of **17**, and synthesis procedures of compounds **23a-d**. This material is available free of charge via the Internet at <http://pubs.acs.org>.

JA072203U